DALTON
FULL PAPER

Conformational choice in disilver cryptates; an ^{1}H NMR and structural study

Oliver W. Howarth,[a] Grace G. Morgan,[b,c] Vickie McKee *[b] and Jane Nelson *[b,c]

[a] *Chemistry Department, University of Warwick, Coventry, UK CV4 7AL*
[b] *School of Chemistry, Queens University, Belfast, UK BT9 5AG*
[c] *Chemistry Department, Open University, Milton Keynes, UK MK7 6AA*

Received 8th February 1999, Accepted 29th April 1999

Disilver complexes of three iminocryptands, with either tris(aminopropylamine)- or tris(aminoethylamine)-derived caps {N[$(CH_2)_n$NCHRCHN$(CH_2)_n$]$_3$N (n = 2 or 3, R = 1,3-$(CH_2)_2C_6H_4$ or 2,5-$(CH_2)_2C_4H_4O$)} have been structurally characterised, and show relatively close approach of the silver(I) ions (3.08–3.77 Å). Differences in the geometry of the coordination site adopted can be related to the flexibility of the cryptand host. This is also important in solution, where the smaller cap-size cryptates are restricted to one conformation while the larger cap-size cryptates appear ready to adopt a range of conformations.

The coordinative plasticity of Ag(I) is of considerable advantage in its role as a templating cation in the assembly of macrocyclic or cryptand ligands. Although the textbook view of Ag(I) is that its preferred mode of coordination is linear two-coordinate, this is not a mode that is commonly found in macrocyclic or cryptate complexes [1–3]. Thus in macrocyclic silver complexes, coordination modes from near square planar to distorted tetrahedral are often found,[1] and higher coordination modes such as pentagonal pyramidal or trigonal bipyramidal occasionally appear.[2] In azacryptates where we have found silver(I) a valuable templating cation, the trigonal pyramidal four-coordinate mode is predominant,[3] but not by any means exclusive. Where steric factors operate, the silver cation shows itself readily satisfied with a coordination number less than four; [4–7] distorted trigonal planar and non-linear two-coordinate geometries have also been observed. The energetic similarity of the alternative coordination environments is well-illustrated in the crystallography of the disilver cryptate of the propylene-capped ligand L^6,[6] where minor and major components of the disorder use respectively: (a) a pair of trigonal pyramidal inclusive sites for both Ag(I) ions, and (b) an unsymmetric conformation where one Ag(I) has this inclusive four-coordinate site while the other occupies a facial three-coordinate site. These Ag(I) cations are separated by a relatively long distance (7.09 or 7.44 Å) where there can be no possibility of a stabilising interaction between the silver ions. In solution, ^{1}H NMR spectra of $[Ag_2L^6]^{2+}$ show fluxionality [8] which may arise, among other things, from interconversion of the conformers in solution.

In the disilver cryptate of an analogous thiophene-linked tris(propylene) (trpn)-capped ligand,[9] ^{1}H NMR studies have shown that two forms are present in solution. The major conformer derives from an unsymmetric pair of coordination sites, despite X-ray crystallographic structure determination which shows the form isolated in the solid state to be symmetric. Once more the separation of coordination sites is large enough to dismiss any chance that interactions between silver(I) cations contribute to the stabilization of particular conformers. Such interactions may exist, however, in disilver cryptates of the small hosts imBT (1,4,7,10,13,16,21,24-octaazabicyclo[8.8.8]-hexacosa-4,6,13,15,21,23-hexaene) and amBT (= imBT + 12 H) where Ag · · · Ag distances of the order of 2.8 Å are observed [4,5] and in other disilver complexes with even shorter Ag · · · Ag distances.[10]

In the light of the increasingly well-demonstrated [11] tendency of Ag(I) cations to aggregate, we wish to examine the solid state structures and solution conformations of our cryptates wherever short internuclear distances between silver(I) ions exist, for comparison with those of dicopper(I) analogues, in an attempt to investigate the relative degree of interaction present in the different d^{10}-d^{10} systems.

Results and discussion

The cryptand hosts, L^1 and L^2 are sufficiently flexible to adopt

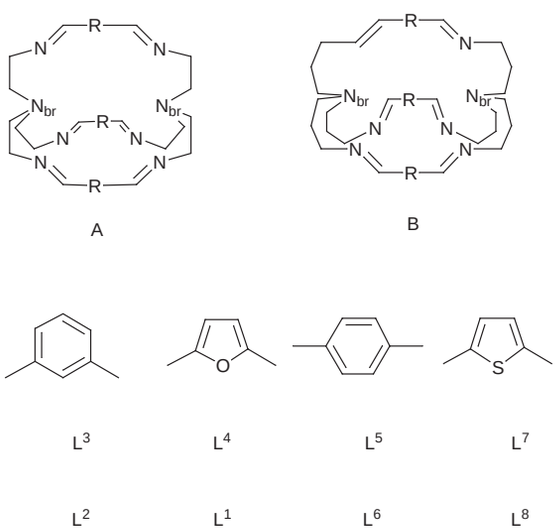

whichever conformation best meets the preferences of the cationic guest. These cryptands were generated by template synthesis on Ag(I), and are isolated as the disilver cryptates $[Ag_2L^1][ClO_4]_2 \cdot 3H_2O$ **1**, and $[Ag_2L^2][ClO_4]_2$ **2**. For comparison, and because few cryptate structures of this ligand were known, the disilver cryptate of L^3, $[Ag_2L^3][BF_4]_2 \cdot 2H_2O$ **3** (made by treatment of the readily available free cryptand with silver tetrafluoroborate) was also synthesised and recrystallised to give X-ray quality crystals.

The ^{1}H NMR spectra of both disilver, **3**, and dicopper, $[Cu_2L^3][(ClO_4)]_2$ **4**, cryptates of L^3 have already been reported,[12] and give no indication of the existence of unsymmetric or additional conformers in solution. The main differ-

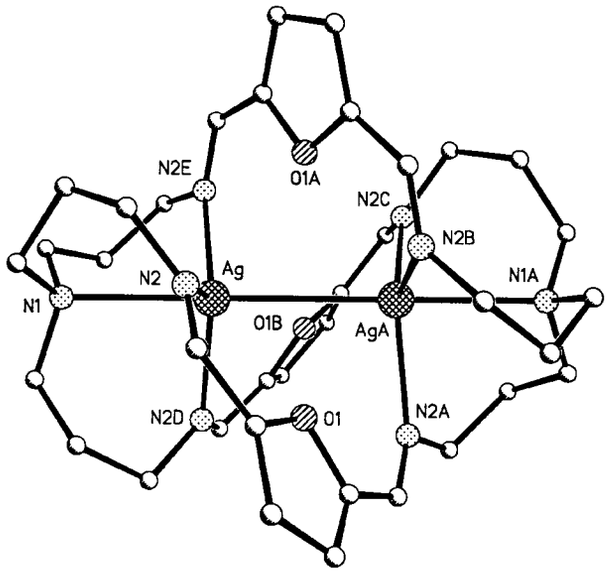

Fig. 1 Structure of $[Ag_2L^1]^{2+}$, **1a**.

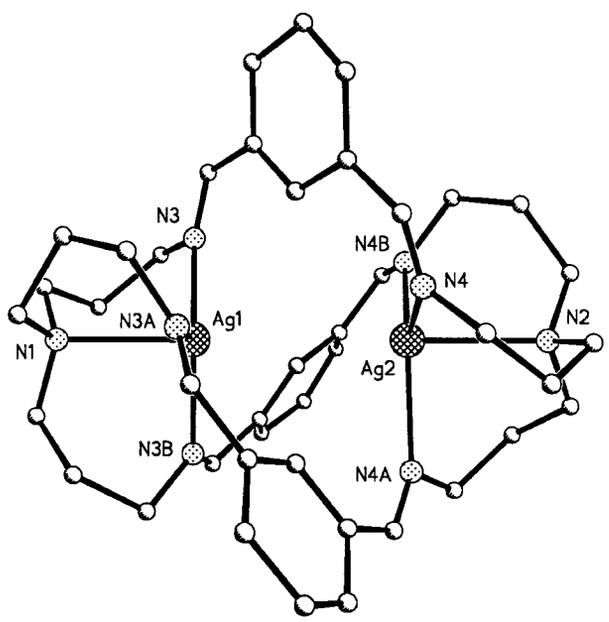

Fig. 2 Structure of $[Ag_2L^2]^{2+}$, **2a**.

ence between the spectra of disilver and dicopper cryptates of this ligand is in the splitting, in **3**, of the (C)H imino signal by coupling $^3J(^1H^{109,107}Ag)$ to the spin-half silver isotopes, which testifies to the absence of rapid exchange on the NMR time scale, between solvated and cryptated situations for the Ag^+ cation.

Although $^{63,65}Cu$–^{15}N coupling is observable[13] in the solid state MAS spectrum, the quadrupolar nature of the copper nuclei prohibits observation, in solution phase spectra, of coupling to the copper nuclei. So information on dynamic exchange processes in solution cannot be derived from ^1H–$^{63,65}Cu$ coupling, but the sharply resolved nature of the ^1H NMR spectrum for **4** suggests the absence of rapid decomplexation equilibria. The crystal structure of the dicopper salt of L^2, **5**, has been described[14] and the well-resolved simple ^1H NMR spectrum, reported for the first time here, suggests that the complex is non-labile and that the solution conformation mirrors that seen in the solid state.

X-Ray crystallographic studies

Suitable crystals for X-ray study of the nitrate salts of $[Ag_2L^1]^{2+}$ **1a** and $[Ag_2L^2]^{2+}$ **2a** were obtained by recrystallisation from ethanol–acetonitrile. These structures are shown in Fig. 1 and 2

Table 1 Selected interatomic distances (Å) and angles (°)

$[Ag_2(L^1)]^{2+}$ **1a**			
Ag–N(1)	2.506(5)	N(2)–Ag–N(2D)[b]	119.04(2)
Ag–N(2)	2.338(3)	N(1)–Ag–N(2)	84.35(6)
Ag–Ag(A)[a]	3.0480(10)		
$[Ag(L^3)]^{2+}$ **3a**			
Ag–N(1)	2.553(2)	N(5)–Ag–N(3)	114.26(9)
Ag–N(5)	2.293(2)	N(3)–Ag–N(4A)[c]	109.21(9)
Ag–N(4A)[c]	2.298(2)	N(5)–Ag–N(4A)[c]	114.46(9)
Ag–N(3)	2.313(2)	N(1)–Ag–N(5)	73.94(8)
Ag–Ag(A)[c]	3.4491(5)	N(1)–Ag–N(4A)[c]	73.57(8)
		N(1)–Ag–N(3)	74.31(8)
$[Ag_2(L^2)]^{2+}$ **2a**			
Ag(1)–N(1)	2.41(3)	N(3)–Ag(1)–N(3A)[d]	119.87(4)
Ag(2)–N(2)	2.43(2)	N(1)–Ag(1)–N(3)	87.9(3)
Ag(1)–N(3)	2.291(12)	N(4)–Ag(2)–N(4A)[d]	119.86(5)
Ag(2)–N(4)	2.358(13)	N(4)–Ag(2)–N(2)	87.8(3)
Ag(1)–Ag(2)	3.775(2)		

Symmetry transformations used to generate equivalent atoms: [a] $y + \frac{1}{3}$, $x - \frac{1}{3}$, $-z + \frac{1}{6}$; [b] $-y + 1$, $x - y$, z; [c] $1 - x$, y, $\frac{1}{2} - z$; [d] $-y$, $x - y$, z.

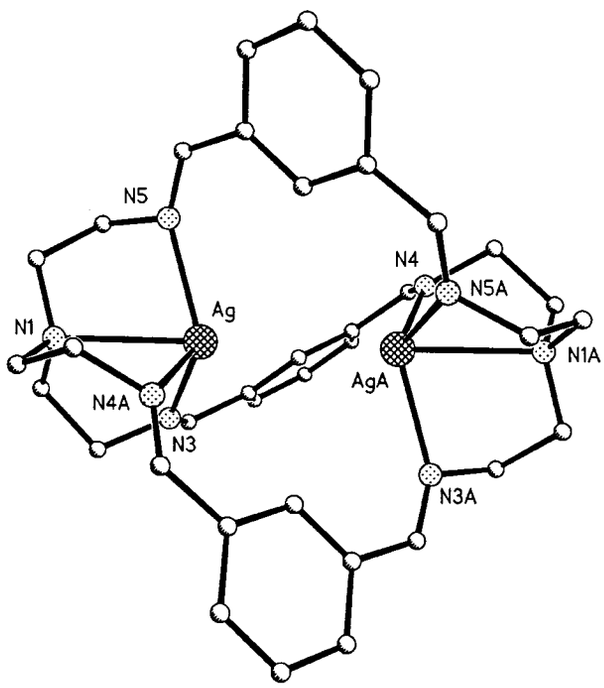

Fig. 3 Structure of $[Ag_2L^3]^{2+}$, **3a**.

and their dimensions are listed in Table 1 together with those of the tetrafluoroborate salt of $[Ag_2L^3]^{2+}\cdot 2MeCN$ **3a** (Fig. 3). Table 2 extends the comparison to include other disilver cryptates structurally characterised to date.

While all three cryptates retain a trigonal pyramidal N_4 cap derived site for Ag^+ coordination, distinct differences between the coordination sites used in tren- and trpn-capped systems are evident. Comparing the thiophene-spaced analogues[9] $[Ag_2L^8]^{2+}$/$[Ag_2L^7]^{2+}$ with the *m*-xylyl-spaced pair of cryptates $[Ag_2L^2]^{2+}$ and $[Ag_2L^3]^{2+}$, we see that in both cases, the tren-derived site presents all four N-atoms well to one side of the cation, the distance from cation to the imino N_3 plane in **3a** being 0.64 Å. In the trpn-derived site of **2a** the Ag^+ cation lies almost coplanar with, *i.e.* within 0.085 Å of, the N_3 plane. The other consequence of the greater flexibility of the trpn cap is that regular trigonal pyramidal angles are achievable within the trigonal plane, and axial to it, in contrast to the tren-capped cryptate **3a** where significant deviations from the ideal 120° and 90° values are seen. The Ag–N distances, however, are not dissimilar for the two cryptates, Ag–N_{imine} falling close to 2.3 Å,

Table 2 Comparisons of dimensions in disilver cryptates[d]

	$[Ag_2L^1]^{2+}$ **1a**	$[Ag_2L^2]^{2+}$ **2a**	$[Ag_2L^3]^{2+}$ **3a**	$[Ag_2L^4]^{2+}$ **6**	$[Ag_2L^5]^{2+}$	$[Ag_2L^6]^{c\,2+}$	$[Ag_2L^7]^{2+}$	$[Ag_2L^8]^{2+}$
Space group	$R\bar{3}c$	$R3c$	$C2/c$	$P2_1/n$	$P2_1/a$	$P\bar{1}$	$P2_1/c$	$P2_1/c$
Ag(1)–Ag(2)/Å	3.05	3.77	3.45	3.11	6.06	7.09	4.65	5.00
N_{br}–N_{br}/Å	8.06	8.61	8.56	8.53	10.85	11.97	9.69	9.96
Ag–X/Å[a]	2.91	2.56	2.65	3.15	2.47	3.15	3.24	3.22
Ag–N_{imine}/Å	2.34	2.31	2.28	2.30	2.31	2.32	2.29	2.31
Ag–imine plane/Å[b]	+0.23	+0.08	+0.64	+0.76	+0.51	−0.23	+0.62	+0.03
Ag–N_{br}/Å	2.51	2.42	2.55	2.68	2.40	2.47	2.68	2.49
N_{im}–**Ag**–N_{im}/°	119.0	119.9	112.6	110.1	115.3	119.5	110.2	119.8

[a] Distance to central hydrogen atom(s) for phenyl spacers, to central O or S atom for the other systems. [b] + Indicates displacement towards central cavity, − indicates displacement towards bridgehead nitrogen atoms. [c] One of the silver ions is disordered over two positions. [d] Average distances given for lower symmetry structures, rounded to two decimal places.

and Ag–N_{br} in the range 2.4–2.7 Å in all cases. The observation of less regular trigonal pyramidal geometry in tren-capped cryptates in comparison with the trpn-derived analogue is general for dinuclear cryptates[8,9,15] and extends even to the analogous podate systems.[16] The Ag···Ag separation in **2a**, at 3.775(2) Å the longest in the disilver L^1–L^4 series, exceeds that in **3a** by ≈0.33 Å and both exceed those in the furan spaced analogues, presumably in response to steric constraints associated with the relatively bulky *m*-xylyl spacer. The relatively long internuclear distance in **2a** would appear to rule out any possibility of Ag···Ag bonding.

Comparing the disilver cryptate $[Ag_2L^1]^{2+}$ **1a** of the furan-spaced trpn-derived $[Ag_2L^4]^{2+}$ ligand, L^1, with its structurally characterised[17] tren-derived L^4 analogue **6**, we see similar effects on the geometry of the coordination site (Table 1). The metal–ligand distances (Ag–N_{imine} at 2.338 for **1a** *vs.* 2.265, 2.326 for **6** and Ag–N_{br} at 2.506 for **1a** *vs.* 2.656, 2.708 Å for **6**) are similar in tren- and trpn-derived cryptates, but the less regular trigonal pyramidal coordination geometry of the tren-derived structure is demonstrated in N–Ag–N angles far from 90°/120° and in the larger Ag–imine plane distances of: 0.713, 0.80 Å for **6** against 0.230 Å for the trpn-capped cryptate, **1a**. The N_{br}–N_{br} distance in **1a** is >0.4 Å shorter than in the tren-capped analogue **6** mainly because of the tighter helical pitch possible in the trpn-capped host. The Ag···Ag distance this time, at 3.048(1) Å is just under 0.07 Å shorter in the trpn-capped cryptate **1a** than in **6**. So in this case, both shorter cavity length and Ag···Ag separation derive in the *larger* host from the increased flexibility which allows the development of a tighter pitch in the triple-helical cryptand strands.

In comparison with the dicopper(I) analogues,[12,14,15,18] M–N_{imine} distances show an expected extension of around 0.25–0.35 Å in the disilver analogues **1a–3a**, where M–N_{br} distances are also longer (by ≈0.1–0.2 Å in the trpn- and 0.2–0.3 Å in the tren-capped pairs). What is less intuitively obvious, however, is that Ag···Ag distances should be markedly *shorter* (by >1 Å) than Cu···Cu distances in the analogous cryptates. This observation contrasts with results for more rigid cryptand hosts studied earlier[9,19] where dicopper(I) and disilver(I) structures are isomorphous or nearly so.

One possible driving force for the M···M contraction in disilver(I) relative to the dicopper(I) cryptates might be the existence, in the silver(I) cryptates only, of Ag–π interactions involving aromatic rings or other, *e.g.* Ag–H, agostic interactions. Table 2 shows that both *p*- and *m*-xylyl-spaced hosts exhibit relatively close approach (of the order of 2.4–2.7 Å between Ag^+ and aromatic protons). However, the contraction of intercationic distances in the *m*-xylyl *versus p*-xylyl spaced analogues is much larger than can be accounted for simply by removal of the additional C–C bond (*i.e.* ≈1.4 Å) in the spacer link. Also, comparison with the dicopper(I) analogues[15,20] reveals similar M–CH_{ar} distances. Although these results appear to rule out indirect interaction as a rationale for the short $Ag^+ \cdots Ag^+$ distances, there remains the hypothesis of direct interaction, of whatever kind, between Ag^+ cations, which is at least conceivable on the results of calorimetric measurements[17] in the Ag–L^4 system, where positive enthalpic cooperativity for complexation of a second Ag^+ cation is exhibited. The enthalpy of complexation of two Ag^+ ions within this host is more (by 13 kJ) than double that for complexation of a single Ag^+ ion. However this 13 kJ excess cannot be interpreted as solely due to $Ag^+ \cdots Ag^+$ interaction as reorganisation costs involved in complexation of the first Ag^+ are likely to be appreciable.

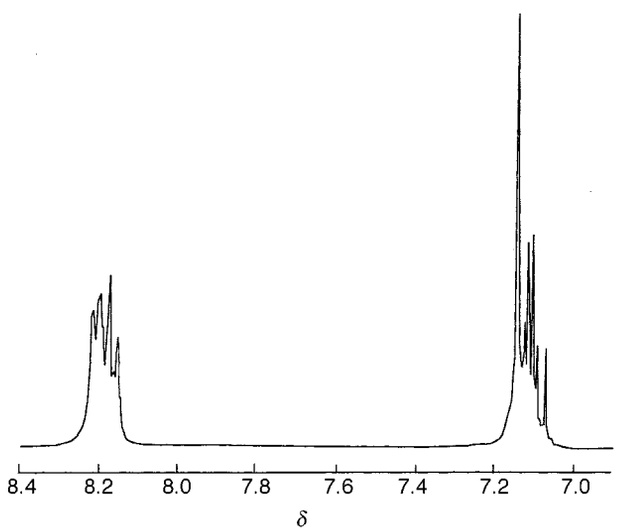

Fig. 4 Aromatic and imino resonances in the δ 7.0–8.5 region of the 400 MHz ^{1}H NMR spectrum of **1** at 230 K.

^{1}H NMR measurements

While the ^{1}H NMR spectra of the dicopper(I) cryptates readily demonstrate that both ends and all strands of the cryptand host are equivalent, the situation with the disilver cryptates is more complex (Table 3). The tren-capped disilver(I) cryptates $[Ag_2L^3]^{2+}$ **3**[12] and $[Ag_2L^4]^{2+}$ **6**,[18] when conformationally frozen out at temperatures below ambient, show simple spectra, suggesting retention of the symmetric solid state conformation in solution. The complexity of the low temperature (233 K) ^{1}H NMR spectra of $[Ag_2L^1]^{2+}$ **1** and $[Ag_2L^2]^{2+}$ **2**, on the other hand, can only be explained by assuming the presence of more than one species in solution for these trpn-capped cryptates.

For $[Ag_2L^1]^{2+}$ **1** (Fig. 4) the appearance of three separate signals in CD_3CN solution in the imino and furano region at 233 K demonstrates the existence of at least three separate conformers. The aromatic resonances consist of two singlets and an AB quartet, the latter suggesting an asymmetric conformation, with inequivalent aromatic protons, while the singlets derive from two different but symmetric dinuclear conformers. The

Table 3 Proton NMR spectra of disilver and dicopper cryptates[g]

Complex	ν/ MHz	T/K	Imino H(C=N)[f]	Aromatic CH	ar_1	Methylene CHs α	β	γ	Ref.
1 major sym	400	230	8.22,d[a] (6.5)	7.14,s[a]	—	[e]	[e]	[e]	This work
1 minor sym	400	230	8.17,d[a′] (7.5)	7.07,d[a′]	—	[e]	[e]	[e]	This work
1 unsym	400	230	8.19,m[a″,h]	7.12,q[a″]	—	[e]	[e]	[e]	This work
2 average	400	298	8.46,d (9.2)	7.80,t;7.78,d;7.73,m	9.92,s	3.35br,s	1.69br,s	2.66;1.90vbr	This work
2 major	400	233	8.42,d (9.4)	7.78,m;7.73,m[b]	9.87,s	3.28,d;2.57,t	1.81,q;[h] 1.68,t[h]	2.99,t;1.70,d	This work
2 minor	400	233	8.47,d (≈9.5)	[e,h]	9.99,s	[e,h]	[e,h]	[e,h]	This work
3	400	233	8.63,d (8.0)	7.84,d;7.76,t	9.59,s	3.51,t;3.31,d	3.08,d;2.65,t	—	12
4	400	233	8.50,s	7.79,d;7.70,t	9.89,s	3.25,m[b]	3.13,d;2.64,m	—	12
5	500	300	8.29,s	7.66,m	10.09,s	3.11,d;3.01,t	2.33,m;[h,c] 1.58,d[c]	2.51,t;1.84,d	This work
6	400	233	8.24,d (7.9)	7.17,s	—	3.54,t;3.19,d	2.96,d;2.55,t	—	9,18

[a,a′,a″] Related *via* NOE enhancement; [b] Not resolvable as separate signals; [c] Related by coupling ($J_{ax,ax'} \approx J_{ax,eq} \approx 15$ Hz). [e] Complex uninterpretable spectra; [f] $^3J(^1H,^{109,107}Ag)$ in parentheses; [g] Shifts in ppm from TMS; s = singlet, d = doublet, t = triplet, q = quartet, m = multiplet; [h] Obscured.

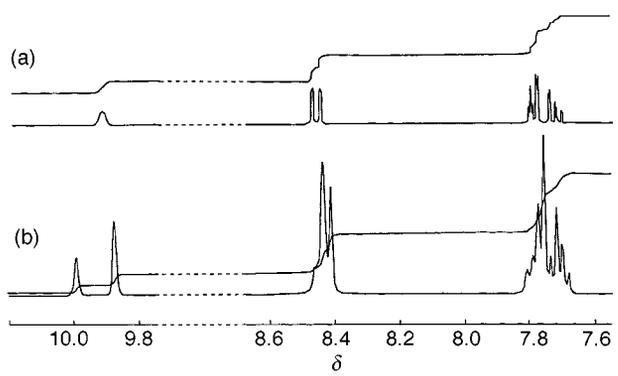

Fig. 5 Aromatic and imino resonances in the 400 MHz ^1H NMR spectrum of **2** at (i) 298 K and (ii) 230 K.

ratio of these different conformers appears as major symmetrical ≈ unsymmetrical ⩾ minor symmetrical. NOE experiments relate the most intense (δ 7.14) furano signal to the δ 8.22 imino doublet having $^3J(^1H,^{109,107}Ag) = 6.5$ Hz (average) and the weak δ 7.07 furano-singlet to the δ 8.17 imino doublet with $^3J(^1H,^{109,107}Ag) = 7.5$ Hz, while irradiation of the quartet at δ 7.12 appears to enhance, though only weakly, imino resonances around δ 8.19. As expected for overlap of three sets of methylene signals, one of them of low symmetry, the methylene region of the spectrum is highly complex and can only be approximately assigned on the data available. NOE and COSY experiments have enabled tentative identification of groups of signals to protons α, β or γ to the imino N in the regions δ 3.5–2.6, ≈1.7 and 2.7–2.3 respectively.

For $[Ag_2L^2]^{2+}$ **2**, also, the complexity of the δ 1.5–4 region of the spectrum discourages attempts at detailed assignment of the methylene protons, at least in the first instance. Instead we initially concentrate on the aromatic and imine regions of the ^1H NMR spectrum. Both ligands L^3 and L^2 contain a unique aromatic proton ar_1, which is subject to the effects of ring currents from aromatic residues in the pair of adjacent cryptand strands. In the tren-capped free ligand, L^3, the relative disposition of ring current with respect to this proton is shielding and accordingly ar_1 appears at δ 5.3, well removed from the normal aromatic region.[21] In the disilver cryptate, **3**, the effect of the ring current on this unique proton is reversed, and the ar_1 resonance is deshielded[12] relative to the normal aromatic range, appearing around δ 9.6. Similar deshielding of ar_1 is observed for $[Ag_2L^2]^{2+}$, **2**, where at 298 K a time-averaged singlet resonance is observed at around δ 9.92, which first broadens as temperature is decreased before freezing out (by 230 K) to a pair of singlets at δ 9.87 and 9.99. Fig. 5 shows the behaviour in the low field (high frequency) region as temperature is varied. The unequal intensity ratio of the resonances points to the presence of a major and a minor solution conformer.

The imino resonance region (δ 8.4–8.5) is consistent with this interpretation, consisting at 233 K of a closely overlapped pair of doublets centred at δ 8.47 and 8.42, with $^3J(^1H,^{109,107}Ag)$ for both close to 9.5 Hz. At 298 K an average coupling between ^1H and $^{109,107}Ag$ of 9.2 Hz is seen; that this coupling persists while the methylene coupling is lost due to time-averaging indicates that the Ag^+ ion remains coordinated during whatever dynamic process is responsible for the loss of coupling in the methylene resonances. The greater $^3J(^1H,^{109,107}Ag)$ coupling in **2** *versus* **1** suggests stronger interaction of Ag^+ with coordinating imino-N in **2**, which does not appear to support any hypothesis of additional Ag^+ involvement in bonding *via e.g.* Ag^+–H_{ar} agostic interaction or incipient $Ag^+ \cdots Ag^+$ bonding.

The remaining aromatic resonances are less easily interpreted, particularly at low temperature. At 298 K doublet and triplet signals around δ 7.8 and a second order multiplet centered around δ 7.7 (arising from a combination of *o*-coupling of around 6 Hz with *m*-coupling close to 2 Hz) correspond to aromatic protons other than ar_1. On freezing out the separate conformers at low temperature, this δ 7.7–7.8 aromatic resonance becomes an overlapped multiplet; however it does not become markedly more complex as might be expected if one of the solution conformers corresponded to an unsymmetrically coordinated situation.

The methylene region of the spectrum at 298 K is broad and fluxional while the 233 K spectrum is once more too complex to be completely assignable, although outline information supported by NOE and COSY experiments allows tentative assignment of resonances due to the major component (Table 3). These assignments are supported by comparison with the spectrum of the dicopper analogue **5** which is relatively simple as it does not suffer from the complication of having more than one conformation in solution.

The evidence of solution NMR studies is that dissolution of the symmetric form of these disilver trpn-capped cryptates results in the generation of additional dinuclear conformer(s), a second symmetric conformer involving a different pair of identical sites, and/or an unsymmetric conformer possibly involving a pair of N_4 (inclusive) and N_3 (facial) coordination sites. However, in neither of the present examples is there evidence for rapid exchange of Ag^+ between the different coordination situations, or with the CD_3CN solvent.

Whatever the rationale for the readiness of the silver(I) cations to approach closely in the solid state, their propensity to adopt other conformations in solution where silver ions may be more widely separated and/or some solvation of Ag^+ may occur, suggests that any Ag · · · Ag interaction cannot exceed by much MeCN solvation enthalpies.

Two (not necessarily mutually exclusive) explanations of the relatively short [*vs.* dicopper(I) analogues] Ag · · · Ag separations present themselves. One is that the larger Ag^+ radius allows for tighter pitch in the triple helical strands than is

Table 4 Data collection and structure refinement parameters

	$[Ag_2(L^1)][NO_3]_2\cdot H_2O$	$[Ag_2(L^3)][BF_4]_2\cdot 2MeCN$	$[Ag_2(L^2)][NO_3]_2$
Formula	$C_{36}H_{60}Ag_2N_{10}O_{13}$	$C_{40}H_{48}Ag_2B_2F_8N_{10}$	$C_{42}H_{54}Ag_2N_{10}O_6$
M	1056.68	1058.24	1010.69
T/K	293(2)	153(2)	293(2)
Crystal system	Rhombohedral	Monoclinic	Rhombohedral
a/Å	15.627(3)	22.869(2)	15.821(3)
b/Å	15.627(3)	11.134(1)	15.821(3)
c/Å	31.583(7)	18.937(2)	34.58(1)
β/°	—	112.520(6)	—
Space group	$R\bar{3}c$	$C2/c$	$R3c$
Z	6	4	6
μ/mm^{-1}	0.951	0.955	0.835
Reflections measured	3011	4466	3309
Independent reflections (R_{int})	1316 (0.0151)	3921 (0.0131)	2957 (0.0530)
Goodness of fit on F^2	1.049	1.044	1.094
Final R indices [$I > 2\sigma(I)$]	$R1 = 0.0281$	$R1 = 0.0282$	$R1 = 0.0635$
	$wR2 = 0.0820$	$wR2 = 0.0618$	$wR2 = 0.1777$
Final R indices (all data)	$R1 = 0.0372$	$R1 = 0.0367$	$R1 = 0.1017$
	$wR2 = 0.0890$	$wR2 = 0.0651$	$wR2 = 0.2088$

possible where the smaller Cu^+ cations are coordinated. The second is that non-zero bond order between the Ag^+ cations is responsible for the relatively close approach. The truth may lie somewhere between these steric and electronic alternatives; we are currently engaged [15] in ADF modelling calculations involving disilver(I) and dicopper(I) cryptates, which will enable us to estimate bond order effects in these different d^{10} cations and thus lead to a better understanding of the observed behaviour.

Conclusion

Two comparisons are emphasised as a result of this study: (i) the difference between tren-capped and trpn-capped hosts, and (ii) the difference between disilver(I) and dicopper(I) cryptates, particularly in respect of cation internuclear distances. In the case of (i), it is seen that the greater flexibility of the trpn-capped ligand allows for adoption of more regular geometry by the encapsulated cations, but this greater flexibility in turn allows competition in solution by several alternative coordination sites for the coordinatively undemanding Ag^+ cation.

In the case of (ii), it appears that the flexible cryptand skeleton, by utilising a triple helical twist mechanism, allows the pair of cations to select from a range of internuclear distances. The separation adopted may derive from steric factors (effect of radius of the coordinated guest on the helical pitch) and/or from electronic effects *viz.* weak bonding between d^{10} systems. In the latter model, $Ag^+\cdots Ag^+$ interactions would appear to be weak but significant in comparison with the $Cu^+\cdots Cu^+$ situation.

Our current modelling studies [15] may explain the origin of the different $d^{10}\cdots d^{10}$ cation separations.

Experimental

Synthesis of cryptates and precursors

Trpn was prepared as described in ref. 22, and used in synthesis of **1**, **2** and **5** as described below. 2,5-Diformylfuran was prepared as described in earlier papers.[18] Isophthalaldehyde was purchased from Aldrich and used as supplied.

$[Ag_2L^1][ClO_4]_2\cdot 3H_2O$ 1. 2,5-Diformylfuran, (0.009 mol) was dissolved in 300 cm^3 methanol and filtered into a dropping funnel. It was added slowly overnight to a solution of silver nitrate (0.006 mol) in methanol (100 cm^3), concurrently with a solution of trpn (0.006 mol) in methanol (300 cm^3) with vigorous stirring at 40 °C. A solution of sodium perchlorate (0.009 mol) in 20 cm^3 methanol was then added dropwise, resulting finally in a beige precipitate. The filtrate was left standing overnight to yield a second crop, and finally reduced in volume on a rotary evaporator to give a third crop. Total yield 73%. FAB-MS *m*/*z* (%): 955 (43) $Ag_2L^1ClO_4^+$; 856 (37) Ag_2L^{1+}; 747 (40) AgL^{1+}. %C H N (calculated percentages in parentheses) C, 39.02 (38.97); H, 4.80 (4.91); N, 10.08 (10.10). The nitrate salt **1a** used for X-ray crystallography constituted the final crop of crystals obtained in this preparation.

$[Ag_2L^2][ClO_4]_2$ 2. Silver nitrate (0.005 mol) and isophthalaldehyde (0.006 mol) were dissolved in methanol (200 cm^3) to give a pinky-brown solution which was stirred at 30 °C for 10 min before trpn (0.004 mol) in methanol (100 cm^3) was added dropwise over 1.5 h, during which time the solution became dark brown. The solution was stirred at room temperature overnight before being filtered to remove the brown-black silver residues, and excess silver perchlorate (0.012 mol) in 80 cm^3 methanol was poured in to produce an instant yellow precipitate which was recovered by gravity filtration. Yield 57%. FAB-MS *m*/*z* (%): 985 (12) $Ag_2L^2ClO_4^+$; 886 (4) Ag_2L^{2+}; 777 (18) AgL^{2+}. %C H N (calculated percentages in parentheses) C, 46.25 (46.47); H, 4.64 (5.01); N, 10.03 (10.32). The sample **2a** used for crystallography was obtained by concentrating the solution from template condensation on silver nitrate, with repeated filtration to remove silver residues.

$[Ag_2L^3][BF_4]_2\cdot 2H_2O$ 3. To 0.001 mol L^3 dissolved in 2 cm^3 $CHCl_3$ was added a solution of 0.002 mol of the silver tetrafluoroborate salt in 6 cm^3 EtOH. A white precipitate was filtered off in around 80% yield which could be recrystallised from acetonitrile; slow evaporation in the dark followed by diethyl ether diffusion yields colorless rhombic crystals suitable for X-ray crystallography. FAB-MS *m*/*z* (%): 693 (100), AgL^3; 802 (30) Ag_2L^{3+}; 889 (15) $Ag_2L^3BF_4^+$. %C H N (calculated percentages in parentheses) C, 42.77 (42.77); H, 4.09 (4.48); N, 11.03 (11.08). The sample **3a** used for crystallography was recrystallised from MeCN by diethyl ether diffusion.

X-Ray crystallography

The data sets were all collected on a Siemens P4 diffractometer using graphite-monochromated Mo-K_α radiation ($\lambda = 0.71073$ Å). $[Ag_2(L^1)][NO_3]_2\cdot H_2O$ and $[Ag_2(L^3)][BF_4]_2\cdot 2MeCN$ were solved by direct methods and $[Ag_2(L^2)][NO_3]_2$ was solved using Patterson methods. All three were refined on F^2 using all the data (ref. 23), full-occupancy non-hydrogen atoms were refined anisotropically and hydrogen atoms were included at calculated positions. The data collection and refinement parameters are listed in Table 4. Although the cations (Fig. 1, 2 and 3) all have

triple helical structures the imposed crystallographic symmetry is different in each case.

The $[Ag_2(L^1)]^{2+}$ cation shows 32 point symmetry, the silver ions lie on the threefold axis and each furan oxygen atom is bisected by a twofold axis. The two nitrate ions associated with each cation are disordered over three equivalent positions on the twofold axes. In $[Ag_2(L^3)][BF_4]_2 \cdot 2MeCN$ the asymmetric unit contains half of the cation, one BF_4^- anion and one acetonitrile solvate molecule. The cation lies on a twofold axis which passes through C(18), C(19) and the mid-point of the Ag–Ag(A) vector. The $[Ag_2(L^2)][NO_3]_2$ structure was initially solved in $R\bar{3}c$ which revealed the cation but not the anions; the nitrate anions were only located in the lower symmetry space group $R3c$. The cation lies on the threefold axis, which passes through the silver ions. As was the case for $[Ag_2(L^1)][NO_3]_2 \cdot H_2O$, the symmetry of the space group requires that the two nitrate ions associated with each cation are disordered over three equivalent positions about the threefold axis but these sites are further disordered. Consequently, each asymmetric unit contains one third of a cation and two thirds of a nitrate ion disordered over two positions.

CCDC reference number 186/1445.

See http://www.rsc.org/suppdata/dt/1999/2097/ for crystallographic files in .cif format.

NMR measurements

^1H NMR spectra were obtained on a Bruker ACP 400 spectrometer, under standard conditions, with acetonitrile-d_3 as solvent. A 2 s presaturation delay was used for NOE-difference spectra. 2D COSY spectra required 256 time-domain points zero filled to 2k × 2k spectrum points after use of sinebell windows.

Acknowledgements

We thank OURC for support (GGM) and EPSRC for access to services, FAB-MS at Swansea, and high field NMR at Warwick.

References

1 S. M. Nelson, *Pure Appl. Chem.*, 1980, **52**, 2461.
2 S. M. Nelson, S. G. McFall, M. G. B. Drew and A. H. bin Othman, *J. Chem. Soc., Chem. Commun.*, 1977, 370; M. G. B. Drew, S. G. McFall, C. P. Waters and S. M. Nelson, *J. Chem. Res.*, 1979, 16.
3 J. Nelson, G. Morgan and V. McKee, *Prog. Inorg. Chem.*, 1998, **47**, 167.
4 J. Coyle, V. McKee and J. Nelson, *Chem. Commun.*, 1998, 709.
5 J. Nelson, V. McKee and R. M. Town, unpublished results.
6 G. G. Morgan, V. McKee and J. Nelson, *Inorg. Chem.*, 1994, **33**, 4427.
7 S.-Y. Yu, Q.-H. Luo, B. Wu, X.-Y. Huang, T.-L. Sheng, X.-T. Wu and D.-X. Wu, *Polyhedron*, 1997, **16**, 453.
8 G. G. Morgan, PhD thesis, Open University, 1996.
9 M. G. B. Drew, O. W. Howarth, G. G. Morgan, D. J. Marrs, C. J. Harding and J. Nelson, *J. Chem. Soc., Dalton Trans.*, 1996, 3021.
10 D. E. Fenton and G. Rossi, *Inorg. Chim. Acta*, 1985, **98**, L29; F. A. Cotton, X. Feng, M. Matusz and R. Poliz, *J. Am. Chem. Soc.*, 1988, **110**, 7077; J. Beck and J. Strahle, *Z. Naturforsch., Teil B*, 1986, 41.
11 P. Pyykko, *Chem. Rev.*, 1997, **97**, 597.
12 Q. Lu, J. F. Malone, V. McKee, N. Martin, C. J. Harding and J. Nelson, *J. Chem. Soc., Dalton Trans.*, 1995, 1739.
13 D. Apperley, S. Coles, W. Clegg, J. Coyle, B. Maubert, N. Martin, V. McKee and J. Nelson, *J. Chem. Soc., Dalton Trans.*, 1999, 229.
14 M. P. Ngwenya, J. Ribenspeis and A. E. Martell, *J. Chem. Soc., Chem. Commun.*, 1990, 1207.
15 M. G. B. Drew, D. Farrell, G. G. Morgan, V. McKee and J. Nelson, unpublished results.
16 J. L. Coyle, PhD thesis, Open University, 1999.
17 R. Abidi, F. Arnaud-Neu, M. G. B. Drew, S. Lahely, D. Marrs, J. Nelson and M.-J. Schwing-Weil, *J. Chem. Soc., Perkin Trans. 2*, 1996, 2747.
18 Q. Lu, J.-M. Latour, C. J. Harding, N. Martin, D. J. Marrs, V. McKee and J. Nelson, *J. Chem. Soc., Dalton Trans.*, 1994, 1471.
19 D. J. Marrs, J. Hunter, C. J. Harding, M. G. B. Drew and J. Nelson, *J. Chem. Soc., Dalton Trans.*, 1992, 3235.
20 M. G. B. Drew, D. McDowell and J. Nelson, *Polyhedron*, 1998, **21**, 2229.
21 D. McDowell, V. McKee, J. Nelson and W. T. Robinson, *Tetrahedron Lett.*, 1987, 7453; M. G. B. Drew, V. Felix, V. McKee, G. G. Morgan and J. Nelson, *Supramol. Chem.*, 1995, **5**, 281.
22 J. Chin, M. Banasczyk, V. Jubian and X. Zou, *J. Am. Chem. Soc.*, 1989, **103**, 4073.
23 G M Sheldrick, SHELXL-97, Universitat Göttingen, 1997.

Paper 9/01041F